MicroRNA expression profiling in the lungs of genetically different Ri chicken lines against the highly pathogenic avian influenza H5N1 virus

MicroRNA profiling in the lungs of H5N1-infected Ri chickens

Sooyeon Lee[1†], Suyeon Kang[1†], Jubi Heo[1], Yeojin Hong[1], Thi Hao Vu[1], Anh Duc Truong[2], Hyun S. Lillehoj[3] and Yeong Ho Hong[1*]

[1]Department of Animal Science and Technology, Chung-Ang University, Anseong 17546, Republic of Korea

[2]Department of Biochemistry and Immunology, National Institute of Veterinary Research, Dong Da, Hanoi 100000, Vietnam

[3]Animal Biosciences and Biotechnology Laboratory, Agricultural Research Services, United States Department of Agriculture, Beltsville, MD 20705, USA.

*Address correspondence to:
Yeong Ho Hong, Ph.D.
Department of Animal Science and Technology
Chung-Ang University, Anseong 17546,
Republic of Korea
Tel: +82-31-670-3025
Fax: +82-31-675-3108
E-mail: yhong@cau.ac.kr

† Both authors contributed equally.

Abstract

The highly pathogenic avian influenza (HPAI) virus triggers infectious diseases, resulting in pulmonary damage and high mortality in domestic poultry worldwide. This study aimed to analyze miRNA expression profiles after infection with the HPAI H5N1 virus in resistant and susceptible lines of Ri chickens.For this purpose, resistant and susceptible lines of Vietnamese Ri chicken were used based on the A/G allele of *Mx* and *BF2* genes. These genes are responsible for innate antiviral activity and were selected to determine differentially expressed (DE) miRNAs in HPAI-infected chicken lines using small RNA sequencing.

A total of 44 miRNAs were differentially expressed after 3 days of infection with the H5N1 virus. Computational program analysis indicated the candidate target genes for differentially expressed (DE) miRNAs to possess significant functions related to cytokines, chemokines, MAPK signaling pathway, ErBb signaling pathway, and Wnt signaling pathway. Several DE miRNA-mRNA matches were suggested to play crucial roles in mediating immune functions against viral evasion.

These results revealed the potential regulatory roles of miRNAs in the immune response of the two Ri chicken lines against HPAI H5N1 virus infection in the lungs.

Keywords: Chicken; Differentially expressed miRNAs; Highly pathogenic avian influenza; H5N1; Lung

INTRODUCTION

Influenza A viruses are negative-sense, single-stranded RNA (-ssRNA) viruses belonging to the *Orthomyxoviridae* family [1]. Influenza A virus infections are the only type of infection in birds [2]. Severe outbreaks of highly pathogenic avian influenza viruses (HPAIVs) have been reported worldwide from 2004 to the present, causing tremendous damage to the poultry industry [3-5]. The HPAI H5N1 virus is a fatal zoonotic disease that occurs in humans and has a mortality rate of approximately 53% [6]. Hemagglutinin (HA) protein binds to the cell and triggers endocytosis to enter the host cell [7]. Moreover, influenza A virus enters the nucleus to replicate the virus [8]. The HPAI H5N1 virus usually infects the trachea, in addition to other organs, especially the lungs, which are a major site of H5N1 replication in chickens [9, 10].

The Vietnamese indigenous Ri chicken, which was used as an experimental animal in this study, is a yellow-fathered Vietnamese poultry [11]. HPAIV-resistant and susceptible lines belonging to the Ri chicken were distinguished by the genotypes of the Mx dynamin-like GTPase (*Mx*) gene and the *BF2* gene, a major histocompatibility complex (MHC) class 1 molecule. Specifically, a substitution at the nucleotide 2032 (amino acid replacement at position 631) of the *Mx* gene allele, from A to G (amino acid serine to asparagine), demonstrated that chickens with allele A (Asn) have antiviral activity, i.e., they are HPAIV-resistant, and chickens with allele G (Ser) lack antiviral activity, i.e., they are HPAIV-susceptible [12, 13]. MHC is a group of genes encoding different structures and functions [14]. Chickens containing the *BF2*-B21 haplotype have a high survival rate and those containing the *BF2*-B13 haplotype have a low survival rate against H5N1 avian influenza virus infection [15].

MicroRNAs (miRNAs) are non-coding endogenous RNAs approximately 22–24 nucleotides in size. miRNAs play various roles, one of which is to regulate gene expression [16]. They function as key regulators of various physiological and cellular activities and immune processes such as immune cell development, differentiation, and activation [17]. Moreover, miRNAs play crucial roles in the immune response of chickens to avian viral infections, such as leukemia, Marek's disease, and infectious bursal disease [18].

A previous study investigated miRNA expression in the thymus, spleen, and bursa of Fabricius of H5N1-infected ducks and White Leghorns via high-throughput RNA sequencing to explore the disparate immunity between ducks and chickens [19]. Moreover, gga-miR-133c, gga-miR-1710, and gga-miR-146c target the *PB1*, *PB1-F2*, and *N40* genes in H5N1-infected chicken lungs [20]. In our previous studies, RNA sequencing revealed

immune-related genes involved in cytokine-cytokine interactions and MAPK signaling pathways in the lung and tracheal tissues of H5N1-infected Vietnamese indigenous Ri chickens [21, 22]. Various cytokines and chemokines are induced by influenza A virus infection and some cytokines are essential for antiviral activity [23]. Highly pathogenic avian influenza virus plays important role in MAPK signaling pathway by modulating MAPKs that have crucial role in innate and adaptive immune response [24].

Although there are studies on the immune function of HPAIV-infected chickens, including miRNA profiling studies, study on miRNA expression profiles between HPAIV-resistant and susceptible lines does not exist. In the present study, we compared differentially expressed (DE) miRNAs in Vietnamese indigenous Ri-resistant and susceptible lines against H5N1 virus infection. In this study, we revealed microRNA expression patterns and the potential of miRNAs that modulate the immune system through the regulation of candidate immune genes in resistant and susceptible lines of chickens infected with the HPAI H5N1 virus.

MATERIALS AND METHODS

Avian influenza virus disease model animals

Twenty specific-pathogen-free (SPF) chickens belonging to 10 resistant and susceptible lines were used in this study (Table 1). The *Mx* and *BF2* genes were used to differentiate between the resistant and susceptible lines. High-resolution melting analysis confirmed the *Mx* gene genotyping results (Fig. S1). The *Mx* gene, which has an adenine (A) at nucleotide 2032, was genotyped as the resistant line of Ri chicken, while the presence of guanidine (G) at this position was genotyped as the susceptible line. Based on *BF2* genotyping, chickens possessing the B21 haplotype were determined to be resistant, and individuals possessing the B13 haplotype were identified as being susceptible. Thus, susceptible line chickens have the *Mx* (G)/B13 haplotype and resistant chickens have the *Mx* (A)/B21 haplotype. Ten 4-week-old Ri chickens (five resistant and five susceptible) were inoculated intranasally with 200 µL of 10^4 50% egg infectious dose (EID50) of A/duck/Vietnam/QB1207/2012 (H5N1), following OIE instructions [25]. Chickens were observed for symptoms of disease daily after infection with the H5N1 influenza virus. All chicken management and experiments were conducted in the Department of Biochemistry and Immunology at the National Institute of Veterinary Research (NIVR), Vietnam (TCVN 8402:2010/TCVN 8400-26:2014).

Tissue collection and total RNA extraction

Lung tissues were collected on day 1 and day 3 from Ri chickens, following the WHO Manual on Animal Influenza Diagnosis and Surveillance. The chickens were euthanized after 1-day and 3-day virus infection. All sterilized lung samples were crushed and completely homogenized by cryogenic grinding in liquid nitrogen. RNAs were extracted from the lung tissue using TRIzol reagent (Invitrogen, Carlsbad, CA, USA) follow by the manufacturer's guidelines. Isolated total RNA was checked for quality using Trinean Dropsense96 (Trinean, Gentbrugge, Belgium) and a Bioanalyzer RNA Chip (Agilent Technologies, Santa Clara, CA, USA).

High-throughput small RNA sequencing

All lung samples, infected and uninfected with HPAIV, were collected (day 1 and day 3 of each 5 samples). In this study, However, based on QC check and RIN values, some samples that did not meet the criteria were excluded (ratio<1 or RIN<7) and samples that passed the quality check were used to sequencing. The miRNA libraries were produced using the TruSeq Small RNA Sample Preparation Kit (Illumina, Inc., San Diego, CA, USA). The microRNA was separated by gel electrophoresis. miRNAs were ligated by their 3′- and 5′-end and then reverse transcribed and expanded to create miRNA libraries. The concentration and distribution of the eluted miRNA library were determined using a Bioanalyzer High-Sensitivity DNA Chip (Agilent Technologies, Santa Clara, CA, USA). The expanded products were sequenced by LAS Company (Gimpo, Republic of Korea) on an Illumina NextSeq 500 System following Illumina's recommended protocol to obtain single-end data of 75 bases.

Analysis of differentially expressed (DE) miRNA

After high-throughput small RNA sequencing, bioinformatic preprocessing and genome mapping were performed. Raw quality bases and adapters were trimmed using Skewer 0.2.2 [26]. The cleaned high-quality reads were mapped to the GRCg6a chicken reference genome, using QuickMIRSeq [27]. All known mature miRNAs and hairpins were obtained from the miRBase (https://www.mirbase.org/). QuickMIRSeq was used to estimate the mapped reads with the reference genome based on miRNA expression levels [27]. The hairpin and miRNA expression values were quantified in units of reads per million (RPM). Between the two selected biological conditions, DE miRNAs were analyzed using edgeR (empirical analysis of DGE in R,

https://bioconductor.org/packages/ release/bioc/html/edgeR.html). DE miRNAs with $\log_2$ fold change (FC)>1 or <-1 with FDR less than 0.05 were considered DE miRNAs.

Recognition and bioinformatic analysis of miRNA target genes

miRNA target genes were predicted to reveal miRNA functions. To predict mRNA targets, miRDB v6.0 (http://mirdb.org/), a miRNA target gene prediction database, was used. Candidate target genes with scores>80 were used for bioinformatic analyses, such as Gene Ontology (GO) and Kyoto Encyclopedia of Genes and Genomes (KEGG) pathway enrichments. GO analyses were analyzed by Gene Ontology Resource (http://geneontology.org/) and GO terms with p-values less than or equal to 0.05 were summarized by REVIGO (http://revigo.irb.hr/). KEGG pathway analysis was analyzed by DAVID (https://david.ncifcrf.gov/summary.jsp).

Validation of miRNA expression using quantitative real-time polymerase chain reaction (qRT-PCR)

Complementary DNA (cDNA) synthesis of miRNAs was conducted using the miScript® II Reverse Transcription Kit (Qiagen, Hilden, Germany) and Mir-X miRNA First-Strand Synthesis Kit (Takara, Kusatsu, Japan), following the manufacturer's protocols. The miRNA cDNAs were used as template for qRT-PCR analysis. miRNA real-time PCR was performed on a LightCycler® 96 (Roche, Basel, Switzerland) and using the miScript® SYBR Green PCR Kit (Qiagen) and Mir-X miRNA qRT-PCR TB Green® Kit (Takara) following the manufacturer's guidelines. Known miRNA primers used for qRT-PCR were derived from the miRNA database miRBase (Table 2). Primers for miRNA were synthesized by Genotech (Daejeon, Republic of Korea). qRT-PCR data were standardized relative to the U1A expression levels. Each qRT-PCR analysis was independently performed three times.

Candidate target gene validation using qRT-PCR

The target gene primers were designed using the NCBI primer design tool (Table 2). The cDNA synthesis process using total RNA was as follows. Total RNA (2 µg) was treated with 2 µL DNase I (Sigma-Aldrich, St. Louis, MO, USA) and incubated at 37 ℃ for 30 min. cDNAs were synthesized using the Revert Aid First Strand cDNA Synthesis kit (Thermo Fisher Scientific, Waltham, MA, USA) following the manufacturer's instructions.

First-strand cDNAs were used as templates for qRT-PCR amplification using AMPIGENE® qPCR Green Mix Lo-ROX (Enzo Life Sciences, Farmingdale, NY, USA) on a LightCycler® 96 System (Roche Life Science). cDNA was added to a mixture including 10 µL 2 × Power SYGR Green Master Mix, 1 µL of each forward and reverse primer, and nuclease-free water up to a total of 20 µL volume. The qRT-PCR results were normalized relative to the expression level of GAPDH. Each qRT-PCR experiment was performed in triplicate.

Statistical analysis

Statistical analyses were conducted using the IBM SPSS software (SPSS 26.0 for Windows; IBM, Chicago, IL, USA). Statistical data were confirmed using the Student's *t*-test, and statistical significance was $p<0.05$. All miRNAs and genes expression levels in the qRT-PCR experiment were calculated using the $2^{-\Delta\Delta Ct}$ method [28]. qRT-PCR was replicated three times, and the mean ± standard error of the mean values for each set were validated.

RESULTS

Sample quality check and miRNA abundance distribution

After H5N1 infection, we observed symptoms such as emphysema and congestive lungs in the chickens. The quality of the 40 lung RNA samples was checked, and small RNA sequencing was performed on 29 samples (Fig. S2). Among them, we focused on the comparison of resistant and susceptible lines after three days of infection with the HPAI H5N1 virus because clear symptoms after H5N1 infection showed at day 3 after infection [i.e., 3 days post-infection (dpi)]. Small RNA sequencing of 13 libraries were performed at an average of approximately 41,323,928 read pairs per library. After trimming and quality checking, 35,833,365 read-pairs, on average, accounted for 90.1 % of the clean read pairs with a Phred score of Q30 (Table S1). After mapping with the chicken reference genome, 16,133,535 reads (51.91%) out of 31,081,156 total reads, on average, belonged to miRNA, whereas the others were hairpin loops (0.13 %), small RNA (5.14 %), mRNA (3.45 %), and unaligned reads (39.37 %) (Table S2).

Identification and characterization of known miRNAs via high throughput small RNA sequencing

DE miRNAs in the lung tissue were described on volcano plots and bar graphs using $\log_2$-fold change ($\log_2$FC) and FDR, which are showed in Table 3 (Fig. 1). We compared the control and infected samples in the resistant and susceptible lines at 3 dpi. We also compared the H5N1 infection samples between resistant and susceptible lines at 3 dpi. The miRNAs with a $\log_2$FC >1 or <-1 and a FDR<0.05 were considered DE miRNAs that are represented as blue dots and red dots in volcano plots. The miRNAs with a $\log_2$FC >1 were denoted to have upregulated expression and those exhibiting a $\log_2$FC <-1 were denoted to have downregulated expression. Total 37 DE miRNAs were expressed in comparison between control and infected samples of 3 dpi resistant lines. The 16 DE miRNAs were upregulated in the infection samples compared control, while 21 DE miRNAs were downregulated. The gga-miR-1731-5p showed the highest $\log_2$FC and gga-miR-1716 showed the lowest $\log_2$FC among 37 DE miRNAs in comparison between control and infected samples of 3 dpi resistant lines (Fig. 1A and B). In addition, there were a total of 32 DE miRNAs between control and infection sample comparisons at 3 dpi in susceptible lines (Fig. 1C and D). The gga-miR-205b showed the highest $\log_2$FC among 12 DE miRNAs and gga-miR-7b showed the lowest $\log_2$FC among 20 DE miRNAs in this comparison group. Moreover, a total of 44 DE miRNAs were expressed in the infection samples between resistant and susceptible lines at 3 dpi (Fig. 1E and F). The 29 DE miRNAs were downregulated in the resistant line compared with the susceptible line, while 15 DE miRNAs were upregulated. In the resistant line, gga-miR-7b, gga-miR-6606-5p, and gga-miR-3537 showed high $\log_2$FC compared to the susceptible line at 3 dpi. Among them, gga-miR-7b showed the highest $\log_2$FC in the resistant line compared to the susceptible line. Furthermore, gga-miR-499-3p and gga-miR-499-5p were downregulated in the resistant line compared to the susceptible line at 3 dpi. Among them, gga-miR-499-3p showed the lowest $\log_2$FC in the resistant line compared to that in the susceptible line.

Bioinformatic analysis of DE miRNA target genes

Hierarchical clustering analysis of 44 DE miRNAs was conducted between the two chicken lines at 3 dpi by the MeV program using Euclidean method (Fig. 2A). The Z-score was used to normalize values based on the expression levels. Moreover, the expression differences between resistant and susceptible could be confirmed through hierarchical clustering. Using miRNA target gene prediction tool miRDB, the target mRNAs of 44 DE miRNAs were predicted a score of 80 or higher. Around 25 GO terms with *p*-value <0.05 were enriched in biological process (BP), molecular function (MF), and cellular component (CC) categories using REVIGO and

visualized by SRplot (Fig. 2B, C, and D) based on gene counts. In BP GO terms, biological process, cellular process, and biological regulation were the most enriched terms. In MF GO terms, molecular function, binding, and protein binding were the most enriched terms. In CC GO terms, cellular component, cellular anatomical entity, and intracellular anatomical structure were the most enriched terms. Moreover, the target genes of the 44 DE miRNAs were involved in 22 KEGG pathways (Fig. 2E). The predicted target genes were involved in various immune-related pathways and signal transduction pathways such as the ErBb signaling pathway, MAPK signaling pathways, TGF-beta signaling pathway, Wnt signaling pathway, and mTOR signaling pathway. Furthermore, the interactions of these eight DE miRNAs and their predicted immune-related target genes were visualized by Cytoscape (Fig. 3). Red circles represent DE miRNAs, and blue rectangular boxes represent target genes. As shown in Fig. 3, various immune-related target genes were modulated by the DE miRNAs, and multiple immune target genes were modulated by more than one miRNA.

Quantitative RT-PCR for DE miRNAs and immune-related target genes

We validated the expression of DE miRNAs in the control and infected samples in the resistant and susceptible lines at 3 dpi via qRT-PCR (Fig. 4). Total of eight miRNAs were selected based on read counts, $\log_2$FC, and target genes. Four miRNAs, gga-miR-34b-3p, gga-miR-9-5p, gga-miR-140-3p, and gga-miR-92-3p, were validated comparison between control and infection in the resistant line at 3 dpi. The gga-miR-34b-3p, gga-miR-9-5p were up-regulated in the infection compared to control in the resistant line at 3 dpi. The gga-miR-140-3p, and gga-miR-92-3p down-regulated in the infection compared to control in the resistant line at 3 dpi. Moreover, four miRNAs gga-miR-34c-3p, gga-miR-205a, gga-miR-1692, and gga-miR-3526, were validated comparison between control and infection at 3 dpi of susceptible line. The gga-miR-34c-3p, gga-miR-205a were up-regulated in the infection compared to control in the susceptible line at 3 dpi. The gga-miR-1692, and gga-miR-3526 were down-regulated in the infection compared to control in the susceptible line at 3 dpi. These miRNAs' immune related target genes were predicted by miRDB (Table 4). We also confirmed the expression of immune related target genes in the infected samples between resistant and susceptible lines at 3 dpi using qRT-PCR. The expressions of gga-miR-34c-3p and the predicted target genes, Ras-related Protein 1B (*RAP1B*) and Grb-associated binder 2 (*GAB2*) were confirmed via qRT-PCR (Fig. 5A). The expression of gga-miR-34c-3p was downregulated in the resistant line compared with that in the susceptible line. And the expression of target genes,

RAP1B and *GAB2* were upregulated in the resistant line. The expression level of gga-miR-92-3p was also downregulated in the resistant line and its target genes dual specificity phosphatase 10 (*DUSP10*) and TNF receptor-associated factor 3 (*TRAF3*) were upregulated (Fig. 5B). In contrast, the expression of gga-miR-9-5p was upregulated in resistant line compared to those in the susceptible line and the expression of target genes, Nuclear factor of activated T cells 3 (*NFATC3*) and, Sm-like protein family 14A (*LSM14A*) were downregulated in resistant line (Fig.5C).

DISCUSSION

In this study, we analyzed miRNA profiles of Ri chickens, in the resistant and susceptible lines infected against HPAI H5N1 virus, using small RNA sequencing. Moreover, we predicted miRNA target genes using miRDB for DE miRNAs. Furthermore, various bioinformatic analysis, such as hierarchical clustering, GO, and KEGG pathway analyses, were conducted for miRNA target genes. The miRNAs and target mRNAs expression levels were validated via qRT-PCR.

The target genes *RAP1B* and *GAB2* were found to be negatively correlated with gga-miR-34c-3p in this study. Expression levels of *RAP1B* and *GAB2* were higher in resistant lines than in susceptible lines. Induction of miR-34c-3p was demonstrated in throat swab samples of H1N1-infected patients [29]. One of the target gene, *RAP1B* is a key signaling node in follicular thyroid carcinogenesis through PKA signaling in mice [30]. Moreover, *RAP1B* plays a crucial role in early T-cell humoral immunity and B-cell development [31]. A previous study suggested that after infection with the H5N1 virus, *RAP1B* expression may be involved in the host immune system by activating the T cell-dependent humoral immune system, B cell development, and biological processes [31]. The other target gene, *GAB2*, plays an important role in cell survival, differentiation, and growth by expressing a protein that interacts with various signaling pathways such as the PI3K, ERK, and JNK signaling pathways [32-36]. Previous studies have suggested that *GAB2* has the potential to play a crucial role in cell immune signal transduction, but the mechanism of *GAB2* in avian influenza infection still requires further research [33, 34, 37]. This study suggests that gga-miR-34c-3p may activates the T cell-dependent humoral immune system, B cell development against avian influenza viruses and interacts with various signaling pathways such as the PI3K, ERK, and JNK signaling pathways by targeting the *GAB2* and *RAP1B* genes after infected with H5N1.

In the present study, gga-miR-92-3p expression was downregulated in the resistant line compared with that in the susceptible line (Fig. 5). The most abundantly founded miRNA in chicken embryo fibroblasts upon H9N2 infection was The gga-miR-92-3p [38]. Moreover, this miRNA was also found in the various macrophage cell line, chicken HD11 and turkey IAH3 [39]. According to qRT-PCR results, gga-miR-92-3p targets *TRAF3* and *DUSP10*. Expression of the immune target genes *DUSP10* and *TRAF3* was higher in the resistant line than in the susceptible line. *DUSP10* (MKP5) is a regulator of MAP kinases such as JNK and p-38 kinases [40]. After influenza virus infection, numerous cytokines and pro-inflammatory cytokines are secreted by MAP kinases, which play a crucial role in the host innate antiviral response. The HPAI H5N1 virus has the potential to induce hypercytokinemia [9]. Therefore, the equilibrium between stimulating cytokine production and inactivating cytokine secretion is crucial to the host immune system. Unlimited secretion of cytokines occur various immune diseases [41]. Moreover, *DUSP10* (MKP5) is also upregulated in avian influenza-infected chicken macrophages [42]. Previous studies suggest that *DUSP10* (MKP5) inactivate cytokines and pro-inflammatory cytokines by inactivating MAP kinases to achieve equilibrium [40, 42]. The other target gene, *TRAF3*, encodes a protein that activates the secretion of type 1 IFNs, such as IFN-α and IFN-β [43]. After infection with the avian influenza virus, TRAF3 interacts with Mitochondrial antiviral signaling protein (MAVS), which is associated with retinoic acid-inducible gene I (RIG-I) signaling against virus infection [44, 45]. After influenza A virus interaction, TRAF3 activates IRF3, IRF7, and NF-κB to stimulate the production of type 1 IFN genes and pro-inflammatory cytokines, which are critical to the host immune response [46]. The present study suggests that gga-miR-92-3p may regulate MAP kinases and activate the secretion of type 1 IFNs as an active immune modulator in response to HPAIV infection by targeting *DUSP10* and *TRAF3*. Moreover, the present study suggests that immune functions were more active in resistant line than in susceptible line through these predicted target genes results.

The gga-miR-9-5p expression was upregulated in the resistant line compared with that in the susceptible line (Fig. 5). According to previous study, gga-miR-9-5p was involved in various signal transduction and immune-related pathways by regulating target genes in the intestinal mucosal layer (IML) of necrotic enteritis (NE)-induced Fayoumi chicken lines [47]. The immune-related target genes of gga-miR-9-5p, *LSM14A* and *NFATC3*, were verified via RT-PCR. These target genes showed negative correlation with gga-miR-9-5p. *LSM14A* expression was higher in the susceptible line compared to resistant line in present study. *LSM14A* contributes to activation of IFN-β in the early period of virus infection [48]. The IFN-β expression was also upregulated in the H5N1 infected susceptible strain of mice compared to resistant [49]. IFN-β activates both pro-inflammatory and

anti-inflammatory cytokines [50]. These reports suggest that gga-miR-9-5p may modulate immune responses such as activation of IFN-β via *LSM14A*. The other target gene *NFATC3* (also known as *NFAT4*) mediates the various cytokines and immune modulatory gene expressions such as IFN-γ and TNF-α [51]. Moreover, *NFAT4* plays a crucial role in the reproduction and survival of T cells [52]. These previous papers suggest that gga-miR-9-5p may mediate cytokines and T cell survival by *NFATC3*. However, since the function of *LSM14A* and *NFATC3* in resistant and susceptible lines infected with AIV has not yet been elucidated, further research is needed. Furthermore, the miR-140-3p was downregulated in the infection sample compared to control in the resistant line at 3 dpi (Fig. 4). Previous study suggested that miR-140-3p regulates TNF-α-induced activation of MAPK and NF-κB by targeting CD38 [53].

Most candidate target genes of DE miRNAs were involved in BP GO terms, comprising biological processes, cellular processes, and metabolic process. Biological processes included the control of gene expression, protein modification, and interaction with proteins or substrate molecules. Cellular components, cellular anatomical entities, and intracellular anatomical structures were the most enriched cellular components obtained through the analysis of the candidate target genes of DE miRNAs upon HPAIV infection. Dendrites were also enriched in GO terms related to cellular components (data not shown). A previous study showed that chicken dendritic cells are involved in inflammation, which is induced during early HPAIV infection, triggering deregulation of the immune response [54]. In addition, dendritic cells participate in the dissemination of the H5N1 virus after the virus escapes viral-specific immunity that leading to cell death [55]. Moreover, various genes that related to the virus life cycle were involved in GO cellular component. The viral ribonucleoproteins (vRNP) gained entry to the host cell nucleoplasm and transported to the nucleus to replicate the influenza virus. After replication, the vRNP complex was exported to the cytoplasm and the plasma membrane for viral assembly. After viral assembly, the influenza virus was released [56].

DE miRNA candidate target genes were involved in various signal transduction and immune-related pathways such as ErbB signaling pathway, MAPK signaling pathway, TGF-beta signaling pathway, and Wnt signaling pathway, and mTOR signaling pathway. Protein synthesis and actin cytoskeleton function in signaling pathways were induced by virus evasion [57]. These were modified upon influenza A virus infection, as observed in LLC-MK2 monkey kidney epithelial cells [58], and A549 human lung adenocarcinoma epithelial cell line [59]. Focal adhesion interacts with PI3K signaling and actin reconstitution after influenza A virus infection [60]. ErbB

signaling pathway modulates immune responses by Interferon –λ and CXCL10 against influenza A virus and Rhinovirus [61]. MAP kinase cascades are triggered upon influenza virus infection [62], which has been demonstrated as a novel approach for the development of antiviral drugs against the influenza virus [63]. MAPK signaling pathway modulates immune responses by regulation of pro-inflammatory cytokines [64]. The epithelial-derived TGF-β suppressed early immune responses during influenza virus infection [65]. The Wnt/β-catenin signaling may improve replication of influenza virus replication [66]. The PI3K/mTOR signaling pathway positively modulates immune cell activation. Moreover, in the dendritic cells, these pathways regulate type I interferon production by activating the interferon-regulatory factor 7 [67]. After infected against H5N1, miRNAs regulate immune responses via these various signaling pathways.

In this study, we compared control and infection samples in resistant and susceptible lines of Ri chickens especially infection samples between resistant and susceptible lines. The 44 DE miRNAs were confirmed to differentially expressed among the H5N1 infected susceptible and resistant lines at 3 dpi. Moreover, GO and KEGG pathway analysis identified their predicted target gene functions. Several DE miRNAs (gga-miR-92-3p, gga-miR-34b-3p, gga-miR-140-3p, gga-miR-205a, gga-miR-9-5p, gga-miR-3526, gga-miR-1692, and gga-miR-34c-3p) and some target genes expressions were validated using qRT-PCR. Therefore, this study revealed the potential regulation of miRNAs that mediate their candidate target genes related to the immune response against HPAIV infection. This may facilitate further studies on the overall understanding of the immune system regulation of miRNAs against HPAIV infection. Moreover, the present study may beneficial to the development of miRNA-based resistant and susceptible biomarkers corresponding to highly pathogenic avian influenza virus infection in poultry.

Authors' contributions

S.L., S.K., A.D.T., H.S.L., and Y.H.H. designed the experiments. S.L., S.K., Y.H., T.H.V., J.H., and A.D.T. performed the experiments. S.L. analyzed the data. S.L., S.K., and Y.H.H. wrote the manuscript. All authors have read and approved the final manuscript.

Competing Interests

The authors declare that they have no competing interests.

Acknowledgements

This study was carried out with the support of the "Cooperative Research Program for Agriculture Science and Technology Development" (Project No. PJ015612), Rural Development Administration and Chung-Ang University Graduate Research Scholarship in 2021, Republic of Korea.

Ethics approval

All experiments and care of chickens were certified by the Ministry of Agriculture and Rural Development of Vietnam (TCVN 8402:2010/TCVN 8400-26:2014).

Availability of data and material

The data presented in this paper are available on request.

Abbreviations

miRNA: micro RNA; AIV: Avian influenza viruses; HPAIV: highly pathogenic avian influenza virus; RAP1B: Ras-related Protein 1B; GAB2: Grb-associated binder 2; TRAF3: TNF receptor-associated factor 3; DUSP10: specificity phosphatase 10; MAVS: Mitochondrial antiviral signaling protein; LSM14A: Sm-like protein family 14A; NFATC3: Nuclear factor of activated T cells 3; RIG-I: retinoic acid-inducible gene I; vRNP: viral ribonucleoproteins.

Additional files

Table S1. Raw reads and clean reads summary of control and HPAI infected samples in the resistant and susceptible lines after 3 days post-infection.

Table S2. Abundant distribution of RNAs in control and HPAI infected samples in the resistant and susceptible lines after 3 days post-infection.

FigS1. *Mx* Chromatograms of Mx gene sequencing results of Ri chicken breed. At polymorphism position (site 2032), only single peak A or G was observed (arrows).

Fig S2. Annotations of **(A)** total and miRNA reads and **(B)** miRNA distributions among different categories of 29 quality checked samples after sequencing from whole samples (Table 1). 29 samples were H5N1-infected and non-infected samples on day 1 and day 3 resistant and susceptible lines. **(A)** Each row represents samples, and the vertical axis represents reads. **(B)** Each category was marked with a different color. The horizontal line represents samples and the vertical axis show the percentage of each category.

REFERENCES

1. Swayne D, Suarez DJRset-oide. Highly pathogenic avian influenza. 2000;19(2):463-75.

2. Capua I, Marangon SJEID. Control of avian influenza in poultry. Emerg Infect Dis. 2006;12(9):1319. https://doi.org/10.3201/eid1209.060430

3. Li K, Guan Y, Wang J, Smith G, Xu K, Duan L, et al. Genesis of a highly pathogenic and potentially pandemic H5N1 influenza virus in eastern Asia. Nature. 2004;430(6996):209-13. https://doi.org/10.1038/nature02746

4. Viseshakul N, Thanawongnuwech R, Amonsin A, Suradhat S, Payungporn S, Keawchareon J, et al. The genome sequence analysis of H5N1 avian influenza A virus isolated from the outbreak among poultry populations in Thailand. Virology. 2004;328(2):169-76.

5. Authority EFS, Prevention ECfD, Control, Influenza EURLfA, Adlhoch C, Fusaro A, et al. Avian influenza overview February–May 2021. EFSA J. 2021;19(12):e06951. https://doi.org/10.2903/j.efsa.2021.6951

6. Lai S, Qin Y, Cowling BJ, Ren X, Wardrop NA, Gilbert M, et al. Global epidemiology of avian influenza A H5N1 virus infection in humans, 1997–2015: a systematic review of individual case data. Lancet Infect Dis. 2016;16(7):e108-e18. https://doi.org/10.1016/S1473-3099(16)00153-5

7. Rust MJ, Lakadamyali M, Zhang F, Zhuang X. Assembly of endocytic machinery around individual influenza viruses during viral entry. Nat Struct Mol Biol. 2004;11(6):567-73. https://doi.org/10.1038/nsmb769

8. Pinto LH, Lamb RA. The M2 proton channels of influenza A and B viruses. J Biol Chem. 2006;281(14):8997-9000. https://doi.org/10.1074/jbc.R500020200

9. To KF, Chan PK, Chan KF, Lee WK, Lam WY, Wong KF, et al. Pathology of fatal human infection associated with avian influenza A H5N1 virus. J Med Virol. 2001;63(3):242-6. https://doi.org/10.1002/1096-9071(200103)63:3<242::AID-JMV1007>3.0.CO;2-N

10. Chamnanpood C, Sanguansermsri D, Pongcharoen S, Sanguansermsri PJSAJoTMPH. Detection of distribution of avian influenza H5N1 virus by immunohistochemistry, chromogenic in situ hybridization and real-time PCR techniques in experimentally infected chickens. Southeast Asian J Trop Med Public Health. 2011;42(2):303.

11. Su V, Thien N, Nhiem D, Ly V, Hai N, Tieu HJAP, Hanoi, Viet Nam. Nguyễn Chí Thành, Lê Thị Thúy, Đặng Vũ Bình, Trần Thị Kim Anh . Đặc điểm sinh học, khả năng sản xuất của. Atlas of farm animal breeds in Vietnam. 2004;3:2-10.

12. Ko J-H, Jin H-K, Asano A, Takada A, Ninomiya A, Kida H, et al. Polymorphisms and the differential antiviral activity of the chicken Mx gene. Genome Res. 2002;12(4):595-601. https://doi.org/10.1101/gr.210702

13. Seyama T, Ko J, Ohe M, Sasaoka N, Okada A, Gomi H, et al. Population research of genetic polymorphism at amino acid position 631 in chicken Mx protein with differential antiviral activity. Biochem Genet. 2006;44(9):432-43. https://doi.org/10.1007/s10528-006-9040-3

14. Kaufman J, Wallny HJI, Chicken DBot. Chicken MHC molecules, disease resistance and the evolutionary origin of birds. Immunoloogy and Developmental Biology of the Chicken. 1996:129-41. https://doi.org/10.1007/978-3-642-80057-3_12

15. Hunt HD, Jadhao S, Swayne DEJAd. Major histocompatibility complex and background genes in chickens influence susceptibility to high pathogenicity avian influenza virus. Avian Dis. 2010;54(s1):572-5. https://doi.org/10.1637/8888-042409-ResNote.1

16. Bartel DPJc. MicroRNAs: target recognition and regulatory functions. Cell. 2009;136(2):215-33. https://doi.org/10.1016/j.cell.2009.01.002

17. Sonkoly E, Ståhle M, Pivarcsi A, editors. MicroRNAs and immunity: novel players in the regulation of normal immune function and inflammation. Semin Cancer Biol; 2008: Elsevier. https://doi.org/10.1016/j.semcancer.2008.01.005

18. Zhou L, Zheng SJJIJoMS. The roles of microRNAs (MiRNAs) in avian response to viral infection and pathogenesis of avian immunosuppressive diseases. Int J Mol Sci. 2019;20(21):5454. https://doi.org/10.3390/ijms20215454

19. Li Z, Zhang J, Su J, Liu Y, Guo J, Zhang Y, et al. MicroRNAs in the immune organs of chickens and ducks indicate divergence of immunity against H5N1 avian influenza. FEBS Lett. 2015;589(4):419-25. https://doi.org/10.1016/j.febslet.2014.12.019

20. Kumar A, Muhasin AV, Raut AA, Sood R, Mishra AJB, insights B. Identification of chicken pulmonary miRNAs targeting PB1, PB1-F2, and N40 genes of highly pathogenic avian influenza virus H5N1 in silico. Bioinform Biol Insights. 2014;8:BBI. S14631. https://doi.org/10.4137/BBI.S14631

21. Vu HT, Hong Y, Truong AD, Lee J, Lee S, Song K-D, et al. Cytokine-cytokine receptor interactions in the highly pathogenic avian influenza H5N1 virus-infected lungs of genetically disparate Ri chicken lines. Anim Biosci. 2022 Mar; 35(3): 367–376. https://doi.org/10.5713/ab.21.0163

22. Vu TH, Hong Y, Truong AD, Lee S, Heo J, Lillehoj HS, et al. The highly pathogenic H5N1 avian influenza virus induces the MAPK signaling pathway in the trachea of two Ri chicken lines. Anim Biosci. 2022 Jul; 35(7): 964–974. https://doi.org/10.5713/ab.21.0420

23. Julkunen I, Sareneva T, Pirhonen J, Ronni T, Melén K, Matikainen S. Molecular pathogenesis of influenza A virus infection and virus-induced regulation of cytokine gene expression. Cytokine Growth Factor. 2001;12(2-3):171-80. https://doi.org/10.1016/S1359-6101(00)00026-5

24. Yu J, Sun X, Goie JYG, Zhang Y. Regulation of Host Immune Responses against Influenza A Virus Infection by Mitogen-Activated Protein Kinases (MAPKs). Microorganisms. 2020;8(7). https://doi.org/10.3390/microorganisms8071067

25. Huprikar J, Rabinowitz SJJovm. A simplified plaque assay for influenza viruses in Madin-Darby kidney (MDCK) cells. J Virol Methods. 1980;1(2):117-20. https://doi.org/10.1016/0166-0934(80)90020-8

26. Jiang H, Lei R, Ding S-W, Zhu SJBb. Skewer: a fast and accurate adapter trimmer for next-generation sequencing paired-end reads. BMC bioinformatics. 2014;15(1):1-12. https://doi.org/10.1186/1471-2105-15-182

27. Zhao S, Gordon W, Du S, Zhang C, He W, Xi L, et al. QuickMIRSeq: a pipeline for quick and accurate quantification of both known miRNAs and isomiRs by jointly processing multiple samples from microRNA sequencing. BMC bioinformatics. 2017;18(1):1-14. https://doi.org/10.1186/s12859-017-1601-4

28. Livak KJ, Schmittgen TD. Analysis of relative gene expression data using real-time quantitative PCR and the 2− ΔΔCT method. Methods. 2001;25(4):402-8. https://doi.org/10.1006/meth.2001.1262

29. Peng F, He J, Loo JFC, Yao J, Shi L, Liu C, et al. Identification of microRNAs in throat swab as the biomarkers for diagnosis of influenza. Int J Med Sci. 2016;13(1):77. https://doi.org/10.7150/ijms.13301

30. Huk DJ, Ashtekar A, Magner A, La Perle K, Kirschner LSJT. Deletion of Rap1b, but not Rap1a or Epac1, Reduces Protein Kinase A–Mediated Thyroid Cancer. Thyroid. 2018;28(9):1153-61. https://doi.org/10.1089/thy.2017.0528

31. Chu H, Awasthi A, White GC, Chrzanowska-Wodnicka M, Malarkannan S. Rap1b Regulates B Cell Development, Homing, and T Cell-Dependent Humoral Immunity. J Immunol. 2008;181(5):3373-83. https://doi.org/10.4049/jimmunol.181.5.3373

32. Pan X-L, Ren R-J, Wang G, Tang H-D, Chen S-DJNb. The Gab2 in signal transduction and its potential role in the pathogenesis of Alzheimer's disease. Neurosci Bull. 2010;26(3):241-6. https://doi.org/10.1007/s12264-010-1109-7

33. Meng S, Chen Z, Munoz-Antonia T, Wu J. Participation of both Gab1 and Gab2 in the activation of the ERK/MAPK pathway by epidermal growth factor. Biochem J. 2005;391(1):143-51. https://doi.org/10.1042/BJ20050229

34. Wöhrle FU, Daly RJ, Brummer TJCC, Signaling. Function, regulation and pathological roles of the Gab/DOS docking proteins. Cell Commun Signal. 2009;7(1):1-28. https://doi.org/10.1186/1478-811X-7-22

35. Gu H, Neel BGJTicb. The 'Gab'in signal transduction. Trends Cell Biol. 2003;13(3):122-30. https://doi.org/10.1016/S0962-8924(03)00002-3

36. Nishida K, Hirano TJCs. The role of Gab family scaffolding adapter proteins in the signal transduction of cytokine and growth factor receptors. Cancer Sci. 2003;94(12):1029-33. https://doi.org/10.1111/j.1349-7006.2003.tb01396.x

37. Pan X-L, Ren R-J, Wang G, Tang H-D, Chen S-D. The Gab2 in signal transduction and its potential role in the pathogenesis of Alzheimer's disease. Neuroscience bulletin. Neurosci bull. 2010;26(3):241-6. https://doi.org/10.1007/s12264-010-1109-7

38. Peng X, Gao Q, Zhou L, Chen Z, Lu S, Huang H, et al. MicroRNAs in avian influenza virus H9N2-infected and non-infected chicken embryo fibroblasts. Genet Mol Res. 2015;14(3):9081-91. http://dx.doi.org/10.4238/2015.August.7.17

39. Yao Y, Charlesworth J, Nair V, Watson MJFig. MicroRNA expression profiles in avian haemopoietic cells. Front Genet. 2013;4:153. https://doi.org/10.3389/fgene.2013.00153

40. Tanoue T, Moriguchi T, Nishida EJJoBC. Molecular cloning and characterization of a novel dual specificity phosphatase, MKP-5. J Biol Chem. 1999;274(28):19949-56. https://doi.org/10.1074/jbc.274.28.19949

41. Salojin KV, Owusu IB, Millerchip KA, Potter M, Platt KA, Oravecz T. Essential role of MAPK phosphatase-1 in the negative control of innate immune responses. Journal Immunol. 2006;176(3):1899-907. https://doi.org/10.4049/jimmunol.176.3.1899

42. Ghosh A. Regulation of proinflammatory cytokiness by map kinase phosphapatase in avian influenza virus infected chicken macrophages. 2011.

43. Wang J, Cheng Y, Wang L, Lin Z, Zhu W, Wang Z, et al. Chicken miR-126-5p Negatively Regulates Antiviral Innate Immunity By Targeting TRAF3. Vet Res. 2021. https://doi.org/10.1186/s13567-022-01098-x

44. Wu B, Peisley A, Tetrault D, Li Z, Egelman EH, Magor KE, et al. Molecular imprinting as a signal-activation mechanism of the viral RNA sensor RIG-I. Mol Cell. 2014;55(4):511-23. https://doi.org/10.1016/j.molcel.2014.06.010

45. Elshina E, Te Velthuis AJJC, Sciences ML. The influenza virus RNA polymerase as an innate immune agonist and antagonist. Cell Mol Life Sci. 2021;78(23):7237-56. https://doi.org/10.1007/s00018-021-03957-w

46. Sun N, Jiang L, Ye M, Wang Y, Wang G, Wan X, et al. TRIM35 mediates protection against influenza infection by activating TRAF3 and degrading viral PB2. Protein Cell. 2020;11(12):894-914. https://doi.org/10.1007/s13238-020-00734-6

47. Rengaraj D, Truong AD, Ban J, Lillehoj HS, Hong YHJA-Ajoas. Distribution and differential expression of microRNAs in the intestinal mucosal layer of necrotic enteritis induced Fayoumi chickens. Asian-Australas J Anim Sci. 2017;30(7):1037. https://doi.org/10.5713/ajas.16.0685

48. Li Y, Chen R, Zhou Q, Xu Z, Li C, Wang S, et al. LSm14A is a processing body-associated sensor of viral nucleic acids that initiates cellular antiviral response in the early phase of viral infection. Proc Natl Acad Sci U S A. 2012;109(29):11770-5. https://doi.org/10.1073/pnas.1203405109

49. Boon AC, DeBeauchamp J, Hollmann A, Luke J, Kotb M, Rowe S, et al. Host genetic variation affects resistance to infection with a highly pathogenic H5N1 influenza A virus in mice. J Virol. 2009;83(20):10417-26. https://doi.org/10.1128/JVI.00514-09

50. Bolívar S, Anfossi R, Humeres C, Vivar R, Boza P, Muñoz C, et al. IFN-β plays both pro-and anti-inflammatory roles in the rat cardiac fibroblast through differential STAT protein activation. Front Pharmacol. 2018;9:1368. https://doi.org/10.3389/fphar.2018.01368

51. Chen J, Amasaki Y, Kamogawa Y, Nagoya M, Arai N, Arai K-i, et al. Role of NFATx (NFAT4/NFATc3) in expression of immunoregulatory genes in murine peripheral CD4+ T cells. J Immunol. 2003;170(6):3109-17. https://doi.org/10.4049/jimmunol.170.6.3109

52. Oukka M, Ho I-C, de la Brousse FC, Hoey T, Grusby MJ, Glimcher LHJI. The transcription factor NFAT4 is involved in the generation and survival of T cells. Immunity. 1998;9(3):295-304. https://doi.org/10.1016/S1074-7613(00)80612-3

53. Jude JA, Dileepan M, Subramanian S, Solway J, Panettieri Jr RA, Walseth TF, et al. miR-140-3p regulation of TNF-α-induced CD38 expression in human airway smooth muscle cells. Am J Physiol-Lung Cell Mol Physiol. 2012;303(5):L460-L8. https://doi.org/10.1152/ajplung.00041.2012

54. Vervelde L, Reemers SS, van Haarlem DA, Post J, Claassen E, Rebel JM, et al. Chicken dendritic cells are susceptible to highly pathogenic avian influenza viruses which induce strong cytokine responses. Dev Comp Immunol. 2013;39(3):198-206. https://doi.org/10.1016/j.dci.2012.10.011

55. Thitithanyanont A, Engering A, Ekchariyawat P, Wiboon-ut S, Limsalakpetch A, Yongvanitchit K, et al. High susceptibility of human dendritic cells to avian influenza H5N1 virus infection and protection by IFN-α and TLR ligands. J Immunol. 2007;179(8):5220-7. https://doi.org/10.4049/jimmunol.179.8.5220

56. Samji TJTYjob, medicine. Influenza A: understanding the viral life cycle. Yale J Biol Med. 2009;82(4):153.

57. Liu N, Song W, Wang P, Lee K, Chan W, Chen H, et al. Proteomics analysis of differential expression of cellular proteins in response to avian H9N2 virus infection in human cells. Proteomics. 2008;8(9):1851-8. https://doi.org/10.1002/pmic.200700757

58. Arcangeletti M, Pinardi F, Missorini S, De Conto F, Conti G, Portincasa P, et al. Modification of cytoskeleton and prosome networks in relation to protein synthesis in influenza A virus-infected LLC-MK2 cells. Virus Res. 1997;51(1):19-34. https://doi.org/10.1016/S0168-1702(97)00074-9

59. Yu G, Liang W, Liu J, Meng D, Wei L, Chai T, et al. Proteomic analysis of differential expression of cellular proteins in response to avian H9N2 virus infection of A549 cells. Front Microbiol. 2016;7:1962. https://doi.org/10.3389/fmicb.2016.01962

60. Elbahesh H, Cline T, Baranovich T, Govorkova EA, Schultz-Cherry S, Russell CJJJov. Novel roles of focal adhesion kinase in cytoplasmic entry and replication of influenza A viruses. J Virol. 2014;88(12):6714-28. https://doi.org/10.1128/JVI.0053

61. Ueki IF, Min-Oo G, Kalinowski A, Ballon-Landa E, Lanier LL, Nadel JA, et al. Respiratory virus–induced EGFR activation suppresses IRF1-dependent interferon λ and antiviral defense in airway epithelium. J. Exp. Med. 2013;210(10):1929-36. https://doi.org/10.1084/jem.20121401

62. Pleschka S, Wolff T, Ehrhardt C, Hobom G, Planz O, Rapp UR, et al. Influenza virus propagation is impaired by inhibition of the Raf/MEK/ERK signalling cascade. Nat Cell Biol. 2001;3(3):301-5. https://doi.org/10.1038/35060098

63. Ludwig SJST. Influenza viruses and MAP kinase cascades–Novel targets for an antiviral intervention? Signal transduction. 2007;7(1):81-8. https://doi.org/10.1002/sita.200600114

64. Xing Z, Cardona CJ, Anunciacion J, Adams S, Dao NJJogv. Roles of the ERK MAPK in the regulation of proinflammatory and apoptotic responses in chicken macrophages infected with H9N2 avian influenza virus. J Gen Virol. 2010;91(2):343-51. https://doi.org/10.1099/vir.0.015578-0

65. Denney L, Branchett W, Gregory LG, Oliver RA, Lloyd CMJMi. Epithelial-derived TGF-β1 acts as a pro-viral factor in the lung during influenza A infection. Mucosal Immunol. 2018;11(2):523-35. https://doi.org/10.1038/mi.2017.77

66. More S, Yang X, Zhu Z, Bamunuarachchi G, Guo Y, Huang C, et al. Regulation of influenza virus replication by Wnt/beta-catenin signaling. PLoS One. 2018;13(1):e0191010. https://doi.org/10.1371/journal.pone.0191010

67. Weichhart T, Säemann MJAotrd. The PI3K/Akt/mTOR pathway in innate immune cells: emerging therapeutic applications. Ann Rheum Dis. 2008;67(Suppl 3):iii70-iii4. http://dx.doi.org/10.1136/ard.2008.098459

Table 1. A number of Vietnamese indigenous Ri chickens in each group.

Sample	Genotype							
Ri chicken (40)	Resistant (*Mx*/A and *BF2*/B21)				Susceptible (*Mx*/G and *BF2*/B13)			
	Control		HPAIV infected		Control		HPAIV infected	
	Day 1	Day 3	Day 1	Day 3	Day 1	Day 3	Day 1	Day 3
	5	5	5	5	5	5	5	5

Table 2. List of primers used in quantitative real-time polymerase chain reaction (qRT-PCR).

miRNA/gene	Forward primer/ Reverse primer	Nucleotide sequences (5'-3')	Accession number
gga-miR-92-3p	F	GGTGGTATTGCACTTGTCCC	MIMAT0001109
gga-miR-9-5p	F	TCTTTGGTTATCTAGCTGTATGA	MIMAT0001195
gga-miR-34c-3p	F	TCTTTGGTTATCTAGCTGTAT GA	MIMAT0026541
gga-miR-205a	F	TCCTTCATTCCACCGGAGTCTG	MIMAT0001184
gga-miR-34b-3p	F	AATCACTAAATTCACTGCCATC	MIMAT0026540
gga-miR-140-3p	F	CCACAGGGTAGAACCACGGAC	MIMAT0003722
gga-miR-3526	F	TTGAAGATGAAGTTGGTGT	MIMAT0016375
gga-miR-1692	F	TGTAGCTCAGTTGGTAGAGT	MIMAT0007584
U1A	F	CTGCATAATTTGTGGTAGTGG	V00444.1
TRAF3	F	CGTCTCGGCGCCACTTAGGA	XM_421378
	R	GGGCAGCCAGACGCAATGTTCA	
DUSP10	F	CCTAGTCCTAAAAGGCGGAC	NM_001031044.1
	R	GATGGACTGAGGTAGTGTGG	
NFATC3	F	AACGAACGGTCTGGTCTTCC	XM_015292362.2
	R	TTGGTGGTAGAGCTTGGCAG	
LSM14A	F	TCTTCATTCCAGTCTGTGGG	NM_001012778.1
	R	GTTAACGAACCTCCTGCAAC	
GAPDH	F	TGCTGCCCAGAACATCATCC	NM_204305
	R	ACGGCAGGTCAGGTCAACAA	
RAP1B	F	TCTAGGTAGCTTGGAGGGGAG	NM_001007852.1
	R	CTGCGCTGATGTTTGGCTTC	
GAB2	F	CCTACGATATTCCCGCCACC	XM_004938929.3
	R	AACCCTAAGCTTTCACCGGG	

Table 3. List of DE miRNAs in the resistant and susceptible lines, as observed at 3 days post-infection. log_2 (FC) means the log2-ratio of the two conditions. log_2 (FC)>1 or <-1 with FDR less than 0.05 were DE miRNAs.

miRNAs	RD3I	SD3I	Log_2FC	FDR
gga-miR-7b	39.626	0.000	12.297	0.000
gga-miR-6606-5p	2.903	0.000	8.545	0.000
gga-miR-3537	0.685	0.066	3.200	0.000
gga-miR-103-2-5p	0.636	0.063	3.171	0.000
gga-miR-193b-5p	0.429	0.096	2.082	0.030
gga-miR-6561-5p	3.058	0.807	1.870	0.000
gga-miR-551-3p	11.481	3.356	1.778	0.000
gga-miR-215-5p	288.454	111.596	1.369	0.000
gga-miR-9-5p	66.432	26.843	1.306	0.000
gga-miR-1648-5p	2.791	1.098	1.299	0.003
gga-miR-460b-5p	3.069	1.257	1.282	0.002
gga-miR-3528	30.284	12.738	1.245	0.000
gga-miR-194	7.636	3.298	1.193	0.001
gga-miR-100-5p	15323.973	6707.018	1.192	0.000
gga-miR-1434	6.670	3.159	1.059	0.004
gga-miR-1456-5p	24.616	51.834	-1.074	0.000
gga-miR-449a	128.744	273.161	-1.086	0.000
gga-miR-455-3p	47.911	102.782	-1.099	0.000
gga-miR-33-3p	25.966	56.417	-1.119	0.000
gga-miR-24-5p	0.526	1.191	-1.135	0.035
gga-miR-184-3p	165.062	374.502	-1.182	0.000
gga-miR-92-3p	6410.386	14666.562	-1.194	0.000
gga-miR-489-3p	13.151	30.452	-1.210	0.000
gga-miR-1788-3p	5.428	13.085	-1.271	0.000
gga-miR-202-5p	0.609	1.519	-1.298	0.007
gga-miR-205a	280.363	691.380	-1.302	0.000
gga-miR-1736-3p	9.930	24.500	-1.309	0.000
gga-miR-449c-5p	192.863	478.195	-1.310	0.000
gga-miR-140-3p	3206.350	8316.880	-1.375	0.000
gga-miR-383-5p	1.349	3.892	-1.490	0.000
gga-miR-1779	0.422	1.219	-1.557	0.003
gga-miR-6557-5p	0.163	0.514	-1.603	0.036
gga-miR-455-5p	63.417	194.496	-1.615	0.000
gga-miR-449b-5p	48.246	153.922	-1.674	0.000
gga-miR-1737	0.250	0.822	-1.694	0.006
gga-miR-6649-5p	0.510	1.857	-1.850	0.000
gga-miR-2954	1554.068	5906.178	-1.926	0.000
gga-miR-460a-3p	0.214	1.060	-2.237	0.000
gga-miR-34c-3p	110.454	564.405	-2.353	0.000
gga-miR-6633-5p	0.036	0.252	-2.633	0.026
gga-miR-490-3p	1.030	7.136	-2.827	0.000
gga-miR-6706-5p	0.124	1.285	-3.330	0.000
gga-miR-499-5p	27.839	534.645	-4.260	0.000
gga-miR-499-3p	0.493	18.895	-5.163	0.000

Table 4. List of predicted immune related target genes of eight DE miRNAs that used for qRT-PCR validation

miRNA	Immune related target genes
gga-miR-9-5p	RBFOX2, SCIN, OXSR1, SIRT1, VAV3, LGMN, PRDM1, CDC73, AP3B1, RNF185, DRD2, PAWR, CD47, HES1, CNOT7, PLEKHA1, FBN1, TRAF3, LSM14A, RUNX2, ONECUT1, MYH9, WASF2, EP300, RAB34, MYO1C, SBNO2, SERINC5, EPAS1, MAEA, NOX4, MAP3K3, PIK3CG, TENM1, STK38, MEF2C, TNC, CLOCK, EMB, GDNF, NEO1, NRP1, PRTG, ADGRA2, LDLRAP1, YBX3, CD200, ARFGEF2, HIPK1, NFATC3, ADAMTS3
gga-miR-34c-3p	FGL1, LSM14A, MITF, FAM49B, RBPJ, PLA2G6, CHD2, RAB8B, GAB2, RAB3C, SLC30A10, MYLK3
gga-miR-92-3p	NR4A3, DENND1B, KMT5B, APPL1, DUSP10, MPP1, TRAF3, FBXW7, LRCH1, WASL, PIK3CD, DUSP1, UBASH3B, RORA, TOB2, ADAM10, KIF5B, RBPJ, NCSTN, SH3PXD2A, NKX2-3, GSN, G3BP2, COL24A1, BCL11B, EPS8, ITGA6, TET2, RUNX2, FAM20C, MYH9, DNAJB9, RAB3C, PTEN, PDGFD, FAM83D, ROR1, DUSP5, LRRK2, HIPK3, EZH2, NPNT, NOX4, MAP2K4, MAP3K20, AGO3, DAGLB, PTPRO, MYCBP2, TRIO, SEMA3A, ROBO2
gga-miR-140-3p	ABL1, IL31RA, LOC771804, SERINC5, DTX3L, PDE5A, FRS2, EPHA4, NEO1, LPL
gga-miR-205a	PRKCZ, RAB11FIP2, CADM1, PIK3R1, RUNX2, TOX, TNFRSF11A, CCL4, LOC107049156, RORA, SPRY1, DUSP7, DUSP8, NRK, PTPRO, ENAH, TANK
gga-miR-3526	SFPQ,PIK3R1,PDE4D,SKIL,CDC42,PAG1,CSMD3,LGI1,HSPA5,CCP110
gga-miR-1692	APIP,ADIPOR2,ITGAV
gga-miR-34b-3p	FAM49B,FGL1,MITF,CHL1,AGR2

Figure legends

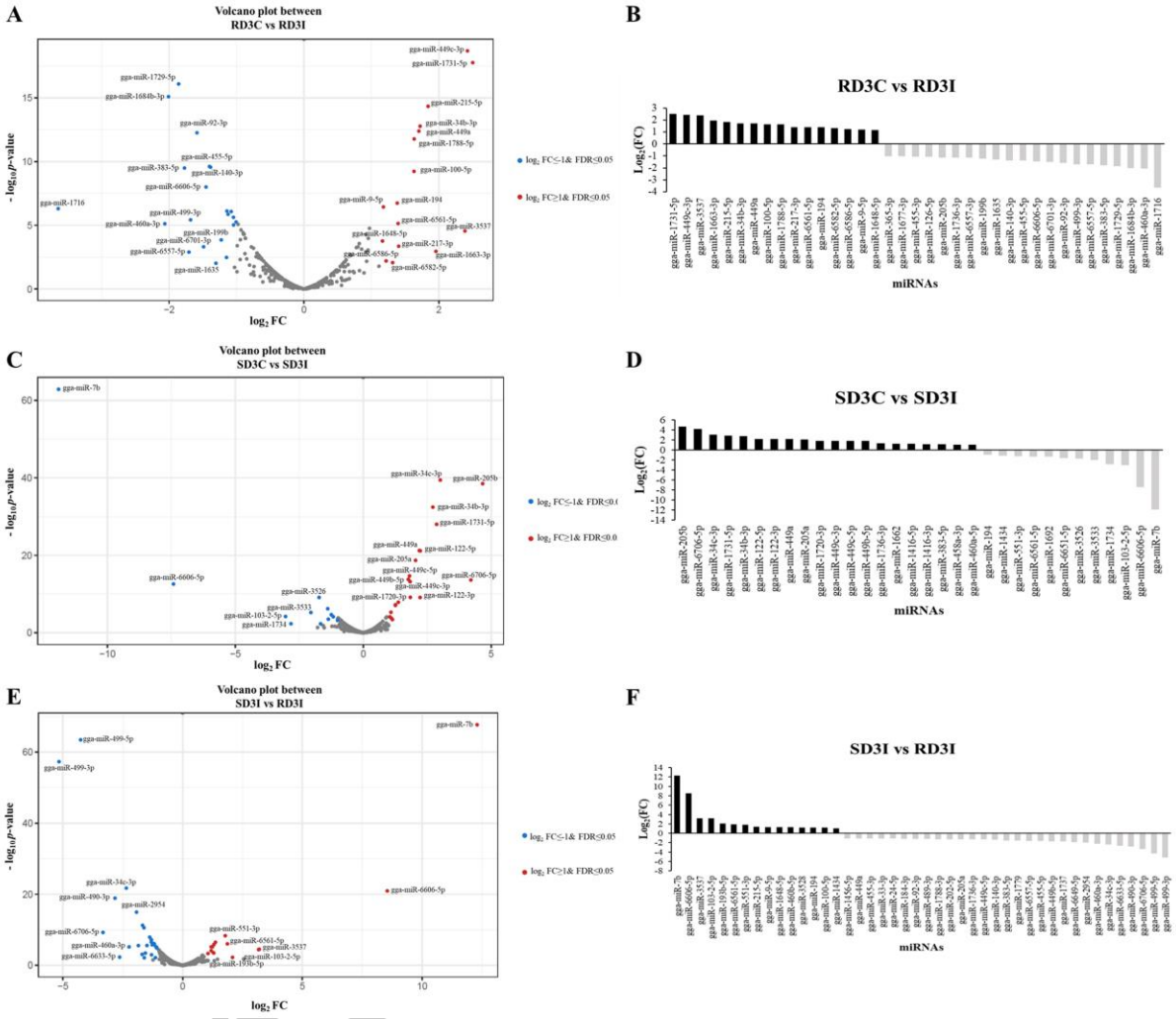

Fig. 1. Volcano plot and bar graph of differentially expressed miRNAs (DE miRNAs). DE miRNAs were represented (A) in the resistant line, (C) susceptible line, and (E) infection samples between the resistant and susceptible lines at 3 days post-infection (dpi). Moreover, miRNAs with an FDR of less than 0.05 and $\log_2$FC over 1 or less than -1 are DE miRNAs marked with blue and red dots, and miRNAs marked with black dots are non-DE miRNAs in volcano plot. DE miRNAs were represented by bar graph. DE miRNAs were represented (B) in the resistant line, (D) susceptible line, and (F) infection samples between in the resistant and susceptible lines at 3 days post-infection (dpi). (B), (D) Black boxes indicated up regulated DE miRNAs in the infection compared to control at 3 dpi. Gray boxes indicated down-regulated DE miRNAs in the control compared to infection at 3

dpi. (F) Black boxes indicated up regulated DE miRNAs in the resistant line compared to susceptible line at 3 dpi. Gray boxes indicated down-regulated DE miRNAs in resistant line compared to susceptible line at 3 dpi.

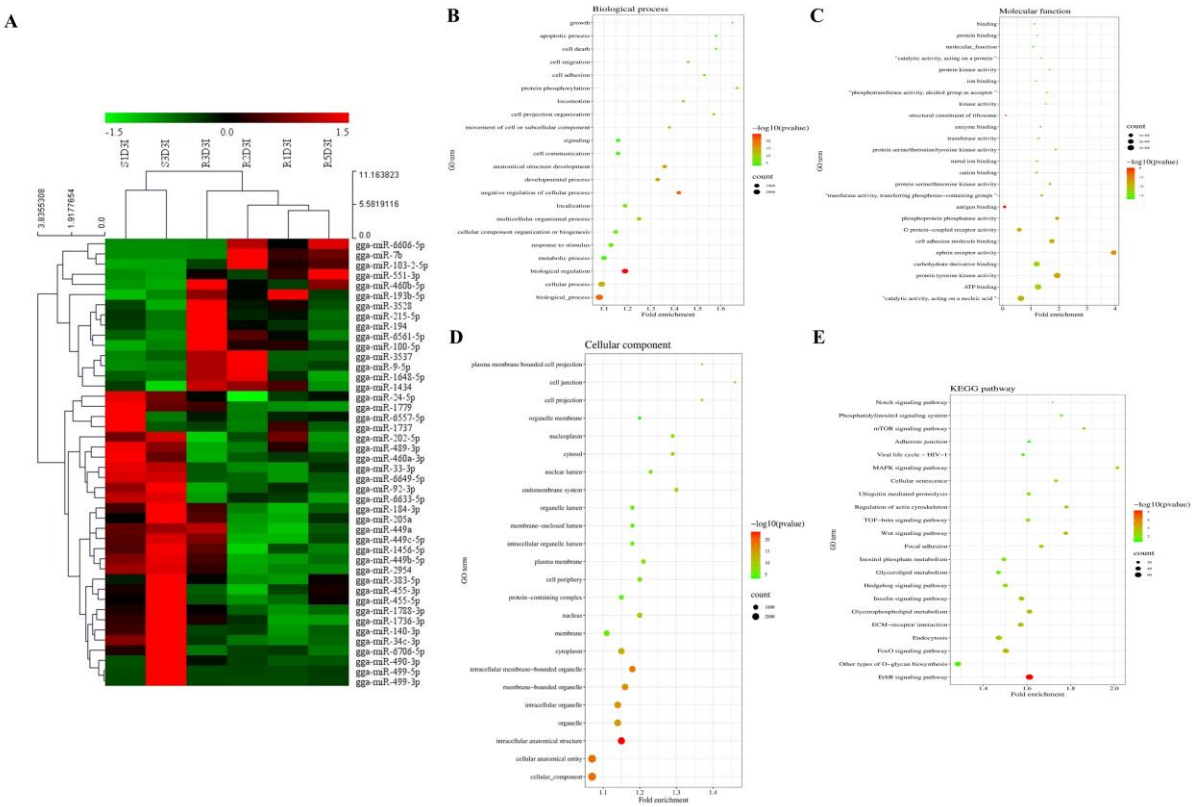

Fig. 2. Hierarchical clustering analysis, gene ontology and KEGG pathway analysis of 44 DE miRNAs. (A) The hierarchical clustering was conducted via MeV program using the Euclidean method in the resistant and susceptible lines at 3 dpi. The red box indicates upregulation, and the green color indicates downregulation. Expression of 29 miRNAs was downregulated in the resistant line compared to that in the susceptible line. However, expression of the other 15 miRNAs was upregulated in the resistant line compared to that in the susceptible line. Z-score was used for normalizing values based on expression levels. (B-E) Gene ontology and KEGG pathway analysis. (B) Biological process, (C) molecular function, (D) Cellular component, and (E) Kyoto Encyclopedia of Genes and Genomes (KEGG) pathway were visualized via SRplot program. The x-axis represents fold enrichment. Color represents −log10 (p-value) and the size of the circle means the number of genes involved in each GO term.

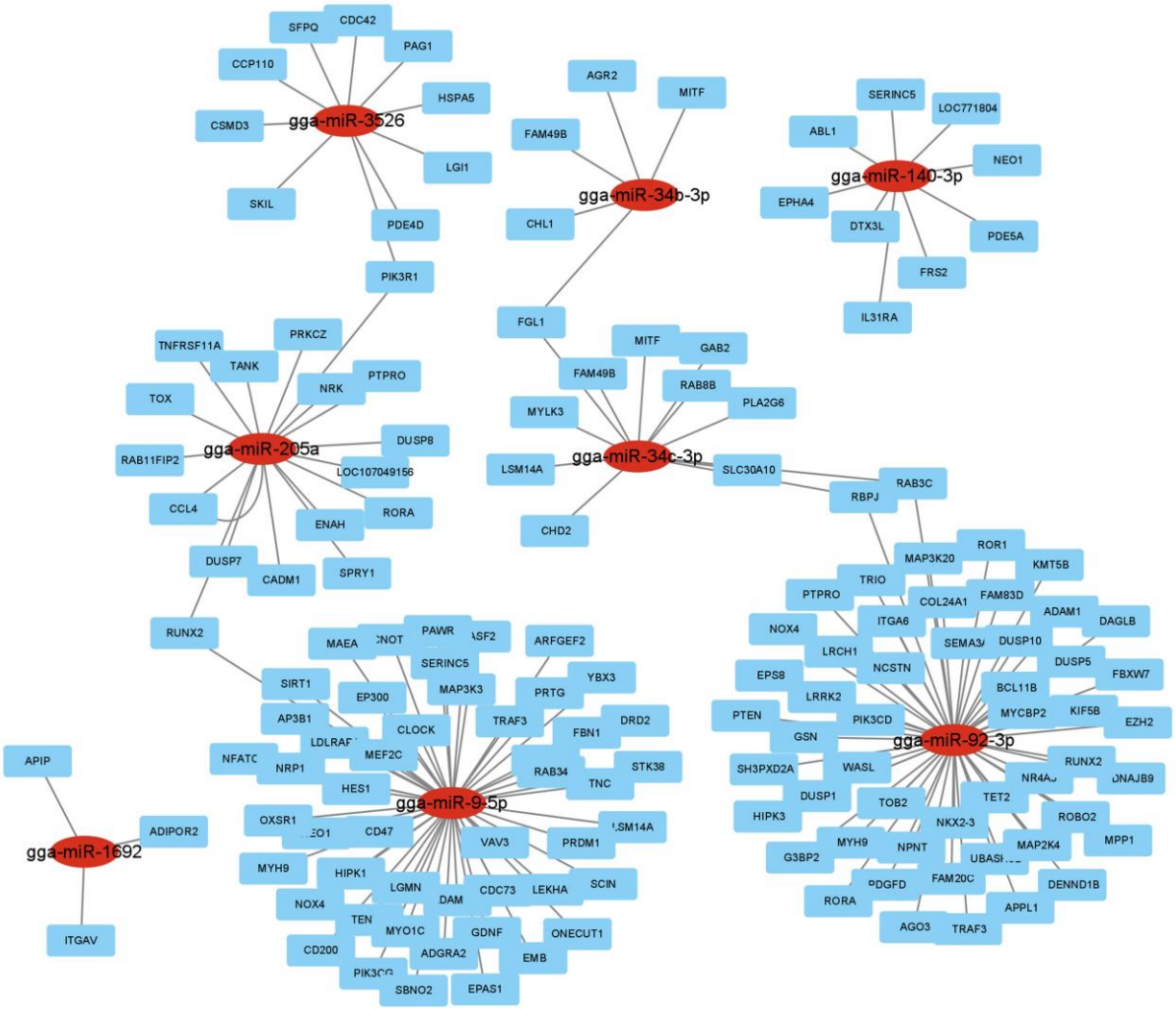

Fig. 3. The interaction of 8 DE miRNAs and their target genes were visualized using the Cytoscape program. The red circle nodes represent each miRNA, and light blue square nodes represent target genes.

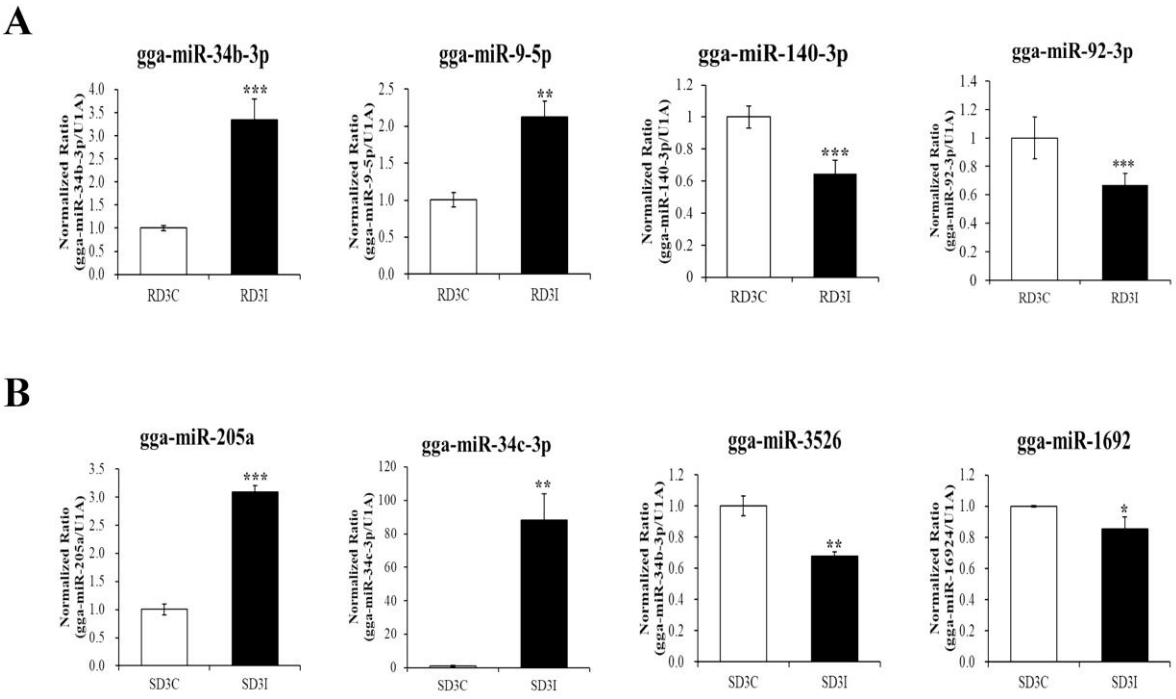

Fig. 4. Quantitative real-time polymerase chain reaction (qRT-PCR) of DE miRNAs between control and HPAI H5N1 infected samples in the resistant and susceptible lines at 3 dpi. Results were normalized to the expression levels of U1A. Significant differences between two comparison groups are indicated as follows: *$p<0.05$, **$p<0.01$, and ***$p<0.001$. Data are presented as the mean ± standard error of the mean of three independent experiments (n=3).

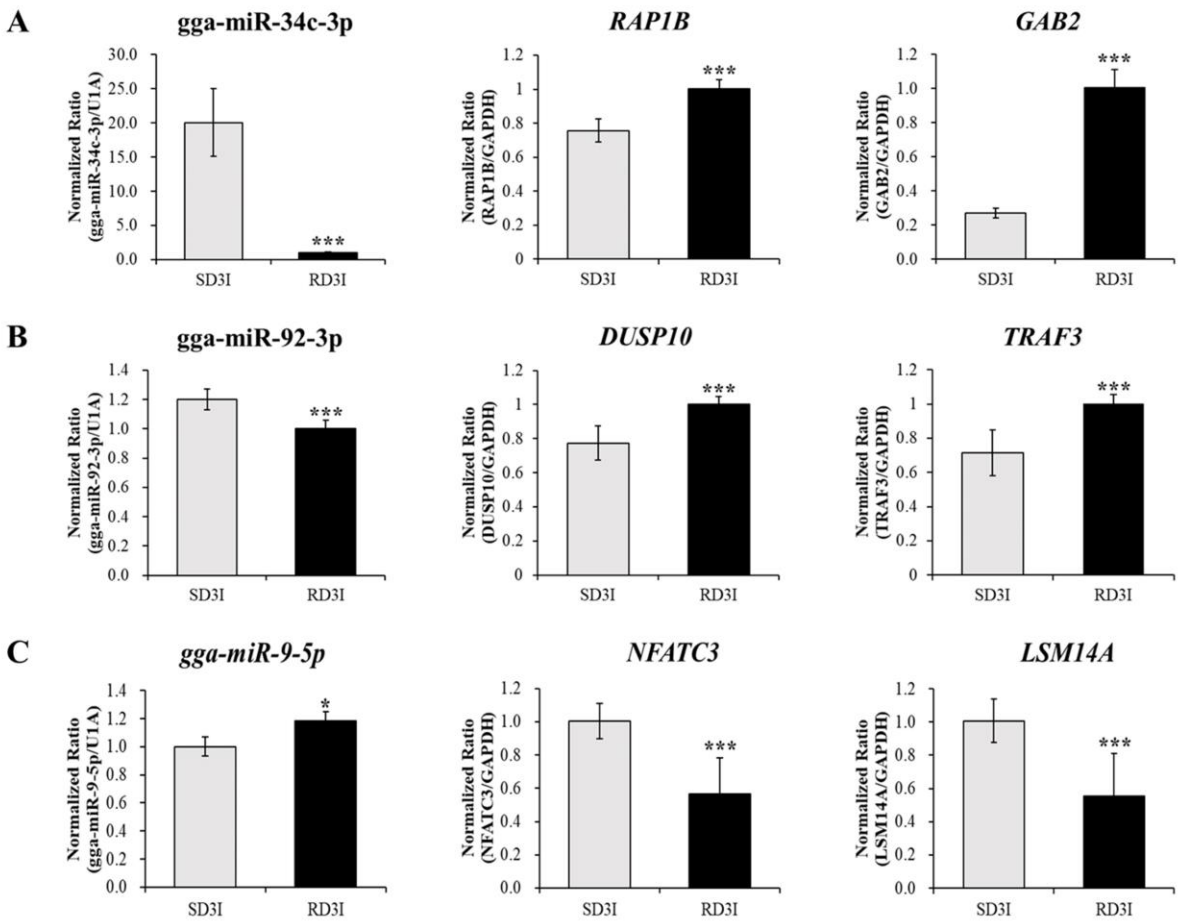

Fig. 5. Quantitative real-time polymerase chain reaction (qRT-PCR) for each miRNA and its target mRNAs between HPAI H5N1 virus-infected susceptible and resistant lines, at 3 days of infection. Results were normalized to the expression levels of U1A (miRNA) or GAPDH (mRNA). Significant differences between two comparison groups are indicated as follows: *p<0.05, **p<0.01, and ***p<0.001. Data are presented as the mean ± standard error of the mean of three independent experiments (n=3).